PART I

BASICS OF MOLECULAR IMAGING AND NANOBIOTECHNOLOGY

CHAPTER 1

Basic Principles of Molecular Imaging

SVEN H. HAUSNER

Department of Biomedical Engineering, University of California–Davis, Davis, California, USA

1.1 INTRODUCTION

The ability to identify diseased tissue for detection and treatment remains a central goal for medical research. Several noninvasive or minimally invasive diagnostic modalities have been developed which allow one to obtain anatomical, physiological, and molecular information. "Molecular imaging" can be defined as in situ visualization, characterization, and measurement of biological processes in the living organism at the molecular or cellular level. Diagnosis and visualization at the molecular level, that is, detection of a disease in its infancy, may significantly improve treatment and patient care. By combining two or more imaging modalities, each with its different strengths, high-quality complementary (e.g., molecular and anatomical) information can be obtained and analyzed in the context of each other. This has led to the rise of dual- and multimodality imaging approaches. Depending on the modality, imaging probes or contrast agents are required or highly desirable; they can range in size from single atoms to cell-sized constructs. Nanoparticles, that is, entities with dimensions in the range of several tens of nanometers, can display desirable pharmacokinetic properties and permit the combination of different clinically relevant moieties (e.g., targeting groups, molecular beacons, and contrast agents for different modalities, surface coatings, enclosed payload) in a single unit. The inclusion of a therapeutic component yields "theranostics." Taken together, nanotechnology-based molecular probes offer the promise for tailor-made clinical tools required for "personalized medicine." This chapter provides an introductory overview of molecular imaging, major imaging modalities, and imaging probes, with particular focus on the promises and challenges of nanoparticle-based compounds.

1.2 IMAGING IN MEDICINE

Most areas of clinical practice require identification and localization of diseased tissue for detection and treatment. Ideally, reliable, specific, and noninvasive high-contrast

Nanoplatform-Based Molecular Imaging Edited by Xiaoyuan Chen

whole-body evaluations would allow physicians to detect serious abnormalities before patients present with symptoms, thus permitting early intervention, thereby increasing the chance for cure or, at a minimum, allow for better patient management and improved quality of life. Given these incentives, it is clear that practical (i.e., minimally inconvenient for the patient) and affordable (i.e., overall cost-saving to the health care system and society) diagnostic approaches are highly desirable. Ever since Wilhelm Röntgen's first use in 1895 of the then newly discovered X-rays to noninvasively image the interior of the body, the keen interest in medical imaging has been met by increasingly sophisticated technologies (Fig. 1.1). While Röntgen's X-ray image was a grainy two-dimensional anatomical projection, physicians nowadays have access to tomographic (three-dimensional) imaging modalities with, depending on the technique, submillimeter resolution, which allows visualization of anatomical, physiological, and, increasingly, molecular (cellular) biological information.

Since diseases often arise from changes on the molecular and cellular levels, long before manifesting themselves in detectable large-scale physiological or anatomical changes, molecular imaging is gaining increasing attention. If a disease can be diagnosed and visualized at the molecular level, that is, detected in its infancy, it can be treated at a much earlier stage, the treatment's efficacy can be determined much sooner and, if necessary, the treatment plan can be adjusted accordingly. This benefits the individual patient and society as a

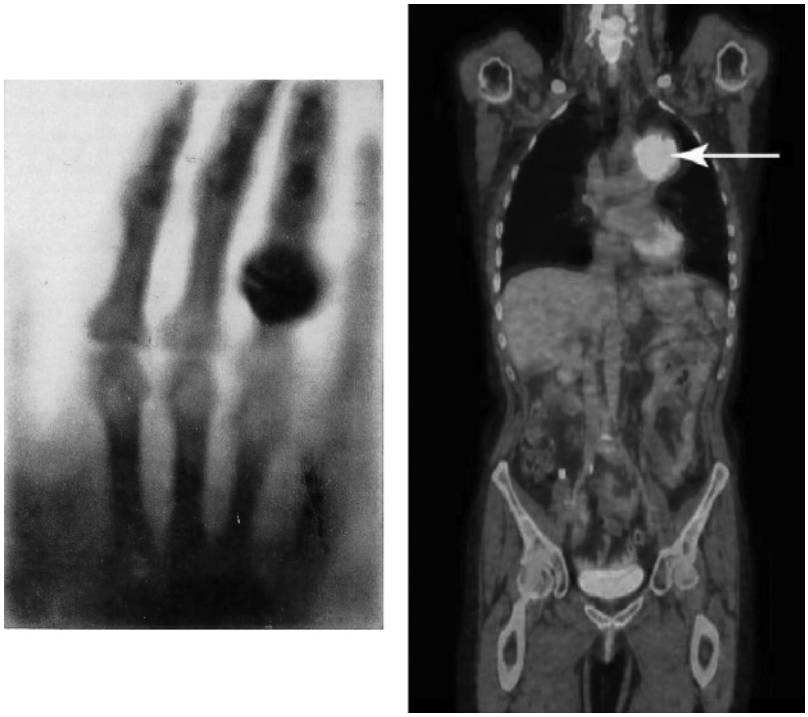

FIGURE 1.1 (Left) Wilhelm Röntgen's (1845–1923) first X-ray image, depicting the hand of his wife, Anna, taken on 22 December 1895. (Right) A slice of a modern whole-body multimodality positron emission tomography/computed tomography (PET/CT) scan showing glucose metabolism within the body, including a large, metabolically active tumor (arrow). (PET/CT image courtesy of Dr. Cameron Foster and Dr. Ramsey Badawi, UC Davis Medical Center, Davis, California.)

whole. Molecular biology is discovering a growing number of disease-specific cellular targets and is determining their distribution in patient populations [1]. For certain diseases this has already had significant effects on determining beforehand which patients will benefit from a certain treatment ("patient stratification"). A prime example is testing for the expression of HER2/neu in breast cancer for prognosis, as well as for selection and monitoring of treatment: expression has been linked to aggressiveness of the disease, but it also provides a target for highly effective treatment with antibodies (Trastuzumab, Herceptin®) [2, 3]. Similarly, monitoring glucose metabolism with the imaging agent ^{18}F-fluorodeoxyglucose (^{18}F-FDG) has proved itself to be the preferred approach for staging, restaging, and evaluation of response to treatment for several cancers [4]. Concurrently with the advances in molecular biology, engineers and physicists are developing increasingly sophisticated imaging instrumentation capable of localizing imaging agents in the body at high sensitivity and high resolution in short acquisition time [5]. By bridging the clinical and engineering worlds, research in imaging agents plays a central role. To that end, the development of target-specific (and disease-specific) nanoparticle-based molecular probes draws on research in several fields including biology, molecular biology, medicine, chemistry, and biomedical engineering.

1.2.1 Molecular Imaging

Rather than relying only on intrinsic large-scale differences of tissue characteristics (e.g., density) or passive accumulation of administered probes to reveal disease *in vivo*, molecular imaging strives to make use of disease-specific ("targeted") interactions of imaging probes with the target tissue on a molecular and a cellular level. The goal is the real-time in situ visualization of biological processes in the living organism. This focus is also reflected in the Society of Nuclear Medicine's definition of molecular imaging as "an array of non-invasive, diagnostic imaging technologies that can create images of both physical and functional aspects of the living body. It can provide information that would otherwise require surgery or other invasive procedures to obtain. Molecular imaging differs from microscopy, which can also produce images at the molecular level, in that microscopy is used on samples of tissue that have been removed from the body, not on tissues still within a living organism. It differs from X-rays and other radiological techniques in that molecular imaging primarily provides information about biological processes (function) while [computed tomography] CT, X-rays, [magnetic resonance imaging] MRI and ultrasound, image physical structure (anatomy)" [6].

As stated above, the information obtained is linked to which imaging modality is chosen. Individual imaging modalities can be grouped by the energy spectrum and energy type evaluated (X-ray, photons, sound; positrons), the resolution that can be achieved, and the type of information obtained (anatomical, physiological, cellular/molecular) (Table 1.1). Widely used clinical imaging modalities include magnetic resonance imaging, ultrasound (US), computed tomography, as well as positron emission tomography (PET) and single photon emission computed tomography (SPECT). All of these modalities allow for the noninvasive imaging of living subjects. Although the first three imaging modalities are primarily *anatomical* and not *molecular*, the two types of modalities can be combined for dual- or multimodality imaging. In addition, MRI, US, and CT *can* be used with molecular imaging probes, especially as part of nanoplatforms. In addition, a number of more specialized optical modalities are being used or are under investigation, including endoscopic methods [12].

TABLE 1.1 Widely Used Imaging Modalities

Imaging Modality[a]	Type[b]	Basis for Detection	Sensitivity (Concentration of Imaging Probe/Contrast Agent)	Resolution	Depth	Quantitative Modality	Typical Scan Acquisition Time	Other
Optical imaging (fluorescence and bioluminescence)	M, P	Fluorescence: External excitation light absorbed by fluorochrome of imaging probe and reemitted at longer wavelength. Bioluminescence: Chemiluminescence of enzymatic reaction.	As low as $\sim 10^{-15}$ mole/L	~1 to ~10 mm	Centimeters	(Yes, limited quantification possible)	Seconds to minutes	Preclinical; limited clinical translation (close to skin or requiring endoscopic approaches) Low cost. Depth limitation based on wavelength-dependent absorption by tissue. Resolution is depth dependent. Two-dimensional (surface) image.
Positron emission tomography (PET)	M, P	511-keV Photons generated during annihilation of positron emitted by radioactive isotope of imaging probe.	$\sim 10^{-11}$–10^{-12} mole/L	1–2 mm (preclinical) 4–8 mm (clinical)	No limit	Yes	Minutes to tens of minutes	Clinical and preclinical. High cost. Versatile imaging probe chemistry.
Single photon emission computed tomography (SPECT)	M, P	Photon emitted by radioactive isotope of imaging probe.	$\sim 10^{-11}$ mole/L [7]	0.5–2 mm (preclinical) 10–15 mm (clinical)	No limit	Yes	Minutes to tens of minutes	Clinical and preclinical. High cost. Versatile imaging probe chemistry. Possibility to distinguish different radioisotopes based on photon energy.

P1: OTA/XYZ P2: ABC
c01 JWBS037-Chen February 2, 2011 21:44 Printer Name: Yet to Come

Magnetic resonance imaging (MRI)	A, P (M)	Interaction of external magnetic field and radiofrequencies with atomic nuclear spins (of tissue or contrast agent) depending on environment of nuclei.	10^{-3}–10^{-4} mole/L	<100 μm (preclinical) <1 mm (clinical) [9]	No limit	Yes	Minutes to hour	Clinical and preclinical. High cost. Long scan acquisition time. Excellent soft tissue contrast.
Ultrasound imaging (US)	A, P (M)	Echoes of tissue (or imaging probe) generated by high-frequency (∼1–40 MHz) sound waves propagating through tissue.	High (single microbubbles—volume ∼0.004 pL—can be detected) [8]	Less than ∼50 μm (preclinical) <500 μm (clinical) [9]	Up to ∼25 cm [10]	Yes	Seconds to minutes	Clinical and preclinical. Low cost. Frequency used determines resolution and (inversely) penetration depth. Targeted imaging limited to vasculature. High operator dependency.
Computed tomography (CT)	A, P	Absorption of focused external X-rays by tissue (or contrast agent).	Low (gram amounts of contrast agent required)	<10 μm (preclinical)	No limit	Yes	Minutes	Clinical and preclinical. Excellent bone and lung contrast. Poor soft-tissue contrast.

[a]Primary molecular imaging modalities are listed in bold.
[b]A, anatomical; M, molecular/cellular; P, physiological.

Source: Adapted from Willmann [11] and Weissleder [12].

Regardless of the imaging modality chosen, quantifiable high-resolution images and reasonable acquisition times are highly desired, and if modalities are combined they should yield relevant additional (e.g., anatomical plus molecular) information. Molecular imaging *per se* is complementary to primarily anatomical imaging (Table 1.1). This is the motivation behind the ongoing push toward dual-/multimodality imaging where molecular imaging data are collected at the same time as anatomical imaging data (Fig. 1.1). This synergistic approach, in which superimposed tomographic images are analyzed, allows the physician interpretation of the molecular imaging data within the anatomical context. The tremendous benefits of this diagnostic approach have also been recognized by the manufacturers of clinical imaging equipment. This has led to the rapid spread of integrated hybrid PET/CT and SPECT/CT scanners in recent years. Dual-modality scanners are now becoming the norm rather than the exception in the clinic [5, 13]. Similarly, hybrid PET/MR scanners are now becoming available; they are eagerly awaited for tasks where the molecular imaging data have to be interpreted in the context of soft tissue, such as, for example, within the brain. Engineering and technical challenges are largely the reason that the availability of hybrid-MR systems has been lagging behind their CT counterparts [14, 15].

The instrumentation for the various modalities has also been adapted for preclinical applications [16]. By using mice, rats, nonhuman primates, or other animal models, specialized small animal scanners allow dedicated imaging in a preclinical research setting. Spatial resolution is generally higher because the subjects can be moved closer to the detectors and the instruments are specifically designed for the reduced dimension required. Because of their small body size, whole-body imaging is easily possible for several species with many of the imaging modalities.

1.3 MAJOR IMAGING MODALITIES

1.3.1 Optical Imaging (Fluorescence and Bioluminescence)

Optical imaging is finding increasing clinical use in several specialized applications, largely using endoscopic (or similar fiberoptic intravital) methods or in regions with limited tissue thickness (e.g., the breast) [12, 17]. Still, the major application of optical imaging lies in preclinical use for small animal studies, chiefly thanks to relatively low cost and simple setup: the subject is placed in a light-tight box and imaged with a highly sensitive charge-coupled device (CCD) camera. A considerable number of optical probes and tags are commercially available, making optical imaging the most popular preclinical imaging modality [5].

For fluorescence imaging the subject is typically illuminated by an external source with excitation light that is absorbed by the fluorophore of an imaging probe. The fluorophore then emits light at lower energies (longer wavelengths) that is detected by the camera. Ideally, the light involved should be in the near-infrared range ($\sim$650–900 nm), where absorbance by blood is minimal. For bioluminescence imaging, no external excitation is required; rather, the faint light emitted by certain biological processes is measured directly. In laboratory studies, this can be achieved by linking a "reporter gene" encoding for a luminescent protein (usually luciferase) to the gene of interest and genetically transferring them into the animal before the study. After administration of an exogenous substrate (e.g., luciferin) light is generated only at sites where the genes are expressed. A similar approach can also be used for modified fluorescence imaging. In this case, the gene for green fluorescent protein (GFP) or one of its derivatives is commonly used as the reporter. Under

illumination, locally expressed GFP emits light that is detected by the CCD camera. An advantage of this approach is the possibility of longitudinal studies because injection of a substrate is not necessary for visualization, whereas the useful window for bioluminescence after a luciferin injection is usually only about 5–30 minutes.

Owing to the fact that a carefully designed optical probe can be switched on and off *in vivo* as a result of chemical or physicochemical transformations, "activatable" or "smart" fluorescent probes have been developed that can respond to the presence and level of biological markers at sites within the body [18]. This has been used in preclinical tumor models to monitor treatment response using a near-infrared fluorophore (NIRF)-based imaging probe responsive to the level of matrix metalloproteinase (MMP)-2. Treatment reduced the level of MMP-2 expressed by the tumor, which was reflected in a reduced signal emitted by the imaging probe.

Several challenges exist for optical imaging. For fluorescence imaging, they include high background signals caused by tissue autofluorescence [19] and limited stability (photobleaching) of many small-molecule fluorophores. Bioluminescence does not have the same problems, but researchers face the tasks of genetically engineering the animal model and detecting very faint signals. Both approaches are constrained by depth limitations due to scattering and absorbance by overlying tissue and the concomitant difficulties with exact quantification. If spatial resolution is not a major concern, whole-body optical imaging is possible for small rodents (especially mice) since scattering and absorption are limited because of the small body size [20].

Perhaps more than for other imaging modalities, a notable number of new approaches based on different technologies are being investigated for optical imaging [12]. Fluorescence lifetime imaging (FLIM), photoaccoustic imaging, multispectral imaging [21], self-illuminating fluorescent imaging probes [19], Raman microscopy techniques, and tomographic fluorescence systems are among the exciting approaches currently under development [12]. Some of them rely entirely on endogenous contrast and do not require the administration of any exogenous probes. Two examples are coherent anti-Stokes Raman scattering (CARS) and optical coherence tomography (OCT). CARS is a nonlinear Raman technique that measures the vibrational spectra of light scattered from illuminated biological specimens. Analysis of the spectra allows conclusions about the constituents of the tissue close to the surface. It has been used *in vivo* to map lipid compartments, protein clusters, and water distribution at subcellular resolution [22]. OCT is a technique based on light scattering that can be described as an optical version of ultrasound (see below). Despite a shallow penetration depth of only about 2–3 mm, it is attractive since it yields real-time very-high resolution (1–15 μm) "optical biopsy" images that are comparable to conventional histopathology. It is finding applications in ophthalmic, gastrointestinal, and intravascular imaging using noninvasive or minimally invasive instrumentation such as handheld probes, endoscopes, catheters, laparoscopes, or needles [23].

1.3.2 Radionuclide-Based Imaging Modalities: Positron Emission Tomography (PET) and Single Photon Emission Computed Tomography (SPECT)

Because of high sensitivity and absence of depth limitations, PET and SPECT are the two molecular imaging modalities that have risen to prominence in both the clinical and preclinical settings. They require the administration of a positron- or single-photon-emitting radioisotope, usually attached to a larger molecule. Examples are [^{18}F]fluorine in

2-[^{18}F]fluoro-2-deoxy-glucose (^{18}F-FDG), [^{123}I]iodine in [^{123}I]metaiodobenzylguanidine (^{123}I-MIBG), or radioactive metal isotopes captured by a chelator (e.g., [^{64}Cu]copper or [^{111}In]indium in chelator-bearing proteins and antibodies). As such, both imaging modalities rely completely on exogenous probes for imaging. For both imaging modalities, the availability, the chemistry, and the radioactive half-life of the chosen isotope have to be considered. This is illustrated by comparing the two popular PET isotopes [^{11}C]carbon and [^{18}F]fluorine. [^{11}C]Carbon is an attractive isotope because it can directly replace a nonradioactive carbon without changing the molecular structure of a compound. However, it has a half-life ($t_{1/2}$) of only 20.4 min, necessitating production in an on-site cyclotron and limiting preparation of the imaging probe to a handful of very fast chemical reactions. By contrast, the nearly 2-h half-life of [^{18}F]fluorine allows a much wider range of chemistries and even some degree of shipment of the imaging probe from central production facilities to outlying hospitals by ground or air. Since the fluorine atom usually takes the place of another element (often a hydrogen atom), possible effects on pharmacokinetics have to be evaluated during drug development. Regardless of which radionuclide-based imaging modality is employed, it is important to use a radioisotope whose physical (radioactive) half-life is matched to the pharmacokinetics of the imaging probe to ensure a sufficiently high signal-to-noise ratio at the time of imaging [24]. Since most nanoparticles have long blood circulation times, it may take up to a few days before the level in the target tissue has risen significantly over background levels. In order to match the long biological half-life of the probe, long-lived radioisotopes are often required. Fortunately, many such radioisotopes are available. For example, the SPECT isotopes [^{123}I]iodine, [^{99m}Tc]technetium, and [^{111}In]indium have half-lives of 13.2 h, 6.0 h, and 67.3 h, respectively, and long-lived PET isotopes include [^{64}Cu]copper, [^{124}I]iodine, and [^{89}Zr]zirconium ($t_{1/2}$ = 12.7 h, 100.2 h, 78.4 h, respectively).

PET, in particular, distinguishes itself through its high sensitivity combined with the ability to image effectively without depth limitation [25]. As mentioned earlier, especially ^{18}F-FDG has helped clinical PET to play a prominent role in cancer detection and monitoring of response to treatment because it allows the visualization of glucose hypermetabolism associated with many malignancies and whole-body PET scans permit the detection of distant metastases (Fig. 1.1). Delicate biological systems (e.g., the brain) can be imaged with minimal disturbance of the molecular processes investigated thanks to the extremely low amount of imaging probe required. The signal detected by the scanner originates from the radioactive decay of a positron-emitting radioisotope prepared in a cyclotron prior to incorporation into the imaging probe. The positron loses energy by scattering through the tissue until undergoing annihilation with an electron, resulting in the emission of two 511-keV photons at an angle of nearly 180°. The pair of photons is detected by a cylindrical array of scintillators connected to photomultiplier tubes (PMTs). Image quality is greatly improved by only accepting valid coincidences and rejecting random events stemming from background radiation: only signals obtained in opposite detectors within a narrow time window, commonly 2–5 ns, are accepted as originating from the same positron-decay event. Resolution-limiting factors are the average range positrons travel before undergoing annihilation ("positron range"), the noncollinearity of the two photons emitted, and detector geometry [26, 27]. The positron range is isotope specific as it depends on the energy with which the positrons are emitted. It can range from $<$1 mm to $>$5 mm for common PET isotopes; for [^{18}F]fluorine it is approximately 0.7 mm [26, 28]. Clinical PET scanners have a typical resolution on the order of several millimeters. Submillimeter resolution is possible

with dedicated small animal scanners, allowing detailed studies of mouse, rat, and monkey models, including brain imaging [25, 29].

Contrary to PET, SPECT directly measures single gamma-ray photons emitted by the decay of the chosen radioisotope. The scanner consists of scintillator/PMT detector heads that slowly rotate around the object in a stepwise fashion, collecting data every few degrees for a certain time. Since only single photons are measured, collimators are used to obtain directional information. Only photons traveling along the axis of the collimator are captured by the detector. This allows SPECT to reach resolutions comparable to PET (Table 1.1), but only at the cost of reduced sensitivity. Depending on the collimator used, sensitivity is reduced by at least about one order of magnitude [7, 11]. On the other hand, since the isotopes commonly used for SPECT have relatively long half-lives on the order of several hours to days, longitudinal studies are greatly facilitated and shipping from distant production facilities is possible. Because of the chemistry of the isotopes involved, straightforward preparation (radiometal chelation) protocols exist for many SPECT imaging probes. In addition, different isotopes can be distinguished based on the isotope-specific energies of the emitted photons (e.g., [^{123}I]iodine: 159 keV; [^{99m}Tc]technetium: 140 keV; or [^{111}In]indium: 171, and 245 keV).

1.3.3 Magnetic Resonance Imaging (MR Imaging or MRI)

MRI is based on the principles of nuclear magnetic resonance (NMR). The nuclei of certain isotopes, most notably naturally occurring hydrogen (i.e., protons), possess nuclear spins that can be aligned along strong external magnetic fields such as those produced inside an MRI scanner. Alignment can be either parallel or antiparallel to the field. Similar to spinning top toys, the spins are not totally aligned with the field but precess around the field vector, resulting in what can be viewed as cone-shaped distributions. Following the application of transverse radiofrequency (rf) pulses to perturb both the longitudinal and transverse alignments, the nuclear spins return to their previous (ground) state, generating a faint signal detected by a receiver coil. Longitudinal (T1 recovery) and transverse (T2 decay) relaxations are measured by the scanner and form the basis for the tomographic image. Relaxation times are dependent on the local environment of the nuclei and on their density within the tissue. Diseased tissue may therefore be detected by its effect on the local density and environment. Furthermore, the rf pulses and their sequence can be modified in order to weight images toward primarily detecting differences in T1 or T2.

Even though protons are virtually ubiquitous throughout the body as part of water and fat molecules, physical limitations, most notably the fact that only a miniscule fraction of spins are aligned properly along the field to generate a signal, result in the relatively low sensitivity of MRI, coupled with long acquisition times (Table 1.1) [11]. Still, MRI is widely used as it permits imaging of soft tissue at high resolution without depth limitation. While images can be acquired by solely relying on native protons (endogenous contrast), the image quality can be greatly improved by administration of certain contrast-enhancing agents. After accumulation in the tissue, these agents change the protons' local environment, thereby shortening their relaxation times (T1 and T2, measured as relaxivities $R1 = 1/T1$, and $R2 = 1/T2$). Gadolinium-chelate-based paramagnetic agents are frequently used to increase T1 contrast, resulting in local brightening in the tomographic image. Newly developed T1 contrast agents include long-circulating manganese oxide (MnO) nanoparticles [30] and gadolinium-containing micelles and liposomes amendable to functionalization [31].

To obtain negative contrast enhancement (darkening) in T2-weighted images, superparamagnetic particles such as iron oxide nanopraticles are typically used. Biocompatibility and ease of synthesis have made colloidal superparamagnetic iron oxide (SPIO) and ultrasmall superparamagnetic iron oxide (USPIO) particles particularly popular. In addition, the continued pursuit of improved magnetic properties has yielded metal-doped ($MnFe_2O_4$, $FeFe_2O_4$, $CoFe_2O_4$, $NiFe_2O_4$), metallic (coated iron, cobalt, nickel), and bimetallic (FePt, FeCo) nanoparticles [32]. Composition, size, surface characteristics, and potential aggregation of the particles, as well as external experimental parameters, all can have an effect on relaxivity and thus the MRI image [32].

Because of the abundance of hydrogen atom within the body, clinical MRI still to a large extent relies on the detection of protons, using contrast agents or high-field MRI scanners to improve contrast [11]. Another way to increase signal strength is to employ hyperpolarized agents. Optical pumping can greatly enrich the excited spin state of certain isotopes (e.g., [^{3}He]helium, [^{129}Xe]xenon), resulting in signal enhancements of up to 10^6 [11]. However, because the hyperpolarized state lasts only a few seconds, the agents need to be prepared immediately prior to imaging and, even then, the time window available for imaging is extremely limited.

In addition to the isotopes mentioned so far, certain isotopes of other elements can be detected as well, provided their natural abundance is high enough (e.g., [^{23}Na]sodium, [^{31}P]phosphorus) or they can be administered in sufficient quantities (e.g., [^{17}O]oxygen as water, [^{13}C]carbon as glucose, [^{19}F]fluorine as fluorocarbons). Because MRI is based on NMR detection, it is possible to tune special scanners to specifically detect spectra of different nuclei. This forms the basis for magnetic resonance spectroscopy (MRS), which is beginning to open the door for quantitative or semiquantitative physiological and molecular MRI by tracing the distribution of individual compounds (e.g., cancer-related metabolites) [33]. To map brain activity, functional MRI (fMRI) detects blood-oxygen-level-dependent changes in the environment of the iron contained in hemoglobin, a measure for the hemodynamic response linked to neural activity. Other novel functional imaging techniques include diffusion-weighted imaging (DWI) and diffusion tensor imaging (DTI) as well as perfusion MRI [33]. DWI and DTI assess the movement of free water molecules in tissue. Perfusion MRI measures blood-transport dynamics by following signal changes with special imaging protocols (dynamic susceptibility contrast MRI, DSC-MRI; dynamic contrast enhanced MRI, DCE-MRI).

1.3.4 Ultrasound (US) Imaging

Ultrasound imaging records the reflections of high-frequency sound waves by internal body structures. Focused sound waves, originating from a transducer placed on the skin, propagate through the body and generate echoes as they encounter tissues of different density. The echoes, in turn, are captured again by the transducer and the data are processed to generate digital images. By performing Doppler sonography, velocity can be measured; this approach is commonly employed for blood-flow examinations. Thus physiology as well as anatomy can be imaged with US [8]. Resolution can be increased by choosing higher frequencies, which, however, lead to a concomitant decrease in penetration depth. Since US imaging does not involve the use of ionizing radiation, it is considered a particularly "safe" imaging modality. Therefore, and because of relatively low cost, ease of use, and wide availability, US is the most popular clinical imaging modality [9]. The image quality depends on sound frequency, sound speed, sound attenuation, sound backscatter, data processing, and

transducer handling [11]. Because of the latter, US imaging is more dependent on the experience and skill of the operator than the other imaging modalities.

Although not necessary for US imaging, contrast agents can be used. Because of their ability to significantly increase the signal intensity, gas-containing microbubbles, along with echogenic liposomes and perofluoro-emulsion nanoparticles, ranging in size from about 100 nm to 8 μm, are most commonly used [8]. They allow for greatly improved imaging of small blood vessels that are otherwise difficult to distinguish from surrounding tissues. Their use, however, is in fact largely limited to imaging the vascular compartment because their particle size precludes escape from blood vessels ("extravasation"). Despite this considerable limitation, clinically approved US contrast agents have been developed and targeted US imaging has been demonstrated with surface-modified microbubbles for diseases that result in molecular changes to the vascular compartment. For example, RGD-peptide modified microbubbles have been used to target the integrin $\alpha_v\beta_3$, a cell-surface receptor linked to tumor angiogenesis [8]. US contrast agents such as microbubbles can also be used for drug delivery. It has been shown that drug-carrying bubbles can be fragmented by high-intensity ultrasound, leading to the local release of a therapeutic agent [34].

1.3.5 Computed Tomography (CT)

For CT a series of X-ray images is acquired and reconstructed into a tomographic image. Focused X-rays emerge from a source rotating stepwise around the subject and, after traveling through the body, are captured by a detector situated opposite the source. Contrast is based on differences in attenuation of the X-rays as they pass through the body. Dense tissue (bones) absorbs significantly more energy than soft tissue, while air (lung) absorbs less. As a result, CT is primarily an anatomical imaging modality that is especially useful for bone and lung imaging but does not show particularly good soft tissue contrast.

For contrast-enhanced CT X-ray absorbing agents are administered. Typically, large amounts of iodine-based compounds have to be administered intravenously to achieve an appreciable soft tissue contrast. The compounds have a largely nonspecific distribution and fast clearance kinetics, although work on improving these characteristics is ongoing [9]. For contrast-enhanced CT of the gastrointestinal tract, insoluble contrast agents based on barium sulfate are given orally or administered as an enema. Recently, lanthanide-bearing compounds, bismuth sulfide nanoparticles, and targeted gold nanorods have been studied as potential future CT contrast agents with increased image contrast and longer circulation times than the standard iodine agents [35–37]. Although CT is just at the verge of also being explored as a molecular imaging modality, it is already extremely useful in providing a high-resolution anatomical framework in which to interpret molecular imaging (e.g., PET or SPECT) data (Fig. 1.1) [13]. The use of PET/CT and SPECT/CT hybrid scanners has improved diagnostic accuracy in the clinic and facilitated preclinical drug evaluation [5].

1.4 MOLECULAR IMAGING PROBES

Even when *ex vivo* diagnostic tests (e.g., blood, urine, Pap smear) exist for a disease [1], the ability to obtain data on location *and* local amount of a disease-specific indicator, and thereby the disease itself, within the body is what makes molecular imaging such a powerful tool. Nowhere is this perhaps more evident than in oncology where tumor heterogeneity, possible involvement of lymph nodes, and the potential of metastases create an extremely

challenging diagnostic target. Detection based on disease-related changes in the local environment provides one possible avenue. This includes imaging of metabolic rate (e.g., glucose consumption), cell proliferation (i.e., DNA synthesis), or a change in the microenvironment (e.g., local pH, concentration of oxygen or proteases) typically associated with cancers. Indeed, a number of small-molecule compounds have been developed into highly successful probes for these conditions, as exemplified by the PET-probes ^{18}F-FDG (for glucose consumption), ^{18}F-FLT (for cell proliferation), and ^{18}F-FMISO or ^{64}Cu-ATSM (for hypoxia) [38]. Even though these probes for local conditions provide very useful information, they still tend to be relatively nonspecific and may miss slow-growing neoplasms [38] or tumors in certain locations such as excretory organs that have a high nonspecific background signal.

Since upregulation of intracellular markers and cell-surface receptors is a hallmark of disease states, aiming for these disease-specific targets is highly attractive, provided that suitable ligands are available. For imaging, cell-surface receptors may be favored over intracellular targets because they do not require internalization into the cell and therefore can be accessed more readily, particularly by nanoparticle-based imaging probes. If the nanoparticle is designed for concomitant drug or gene delivery, subsequent internalization into the cells becomes important. Giving examples from oncology, Table 1.2 illustrates the range of receptor targets and targeting ligands presently available. The examples are taken from MRI imaging [39], but are equally representative for other molecular imaging modalities [12, 18, 38, 40].

Most imaging probes are administered intravenously and allowed to distribute through the body; Notable exceptions include experimental implantable microprobes containing nanoparticles [41], intrinsically produced optical imaging probes (i.e., fluorescent or bioluminescent proteins [42]) expressed by reporter genes, and locally injected imaging probes for sentinel lymph node mapping during cancer surgery [43]. Typically, as the individual probes circulate through the body they can accumulate in tissues, be excreted from the body, and/or be metabolized. To be clinically useful, molecular imaging probes should be based on high-affinity high-specificity ligands and show a relatively low background signal [44]. The ratio of imaging probe in the target tissue versus in the surrounding tissues (i.e., the signal-to-noise ratio) determines how much image contrast can be achieved. In other words, the image depends on how well the imaging probe has been taken up in the target tissue and how well it has cleared from other regions of the body at the time the image is acquired. Therefore some uptake period is frequently required between injection and imaging. Depending on the desired information and the pharmacokinetics of the imaging probe, it can range from a very short time (e.g., seconds to minutes for [^{15}O]oxygen-water in blood flow studies [45] to over tens of minutes (e.g., for ^{18}F-FDG) to days (e.g., for antibodies). Size has a significant impact on the time imaging probes circulate in the body. Generally, small molecules are eliminated fast, resulting in a rapidly decreasing background signal, while larger compounds, including nanoparticles [46], have longer circulation times. Thus, as outlined earlier, for radionuclide-based imaging the radioactive half-life of the radioisotope has to be matched to the pharmacokinetic profile of the imaging probe to ensure that a sufficient radioactive signal remains by the time an adequate amount of the imaging probe has accumulated in the target tissue in order to obtain statistically significant contrast. For nanoparticles this usually requires radioisotopes with half-lives on the order of several hours to days. Algorithms help to choose radioisotopes with an appropriate half-life: by calculating a suitable "imaging figure of merit" (IFOM) that takes into account parameters such as the size of the target organ (or tumor), the measured decay corrected organ uptake (% injected

TABLE 1.2 Targeted Iron Oxide Nanoparticles for Tumor Imaging with MRI

Iron Oxide Nanoparticles	Targeting Ligands	Targets	Tumor	Experimental Conditions
USPIO	Monoclonal antibody-610	Surface antigen	Colon carcinoma cell lines	*In vitro*
SPIO	Antibody to carcinoembryonic antigen (CEA)	CEA	Colon tumor	*In vivo*
MINO	Monoclonal antibody L6	Surface antigen	Intracranial tumor LX-1	*In vivo*
USPIO	Transferrin	Transferrin receptor	Rat mammary carcinoma	*In vivo*
Streptavidin-conjugated SPIO	Monoclonal antibody-Her-2/neu	Her-2/neu receptors	Breast cancer	*In vitro*
CLIO-NH_2	EPPT peptide	Underglycosylated mucin-1 antigen (uMUC-1)	Breast, colon, pancreas, and lung cancer cell lines	*In vivo*
Dextran-coated superparamagnetic maghemite (γ-Fe_2O_3) nanocrystals	Folic acid	Folate receptor	Human epithelial mouth carcinoma	*In vitro*
Ferumoxides (SPIO)	Monoclonal antibody A7	Colorectal tumor antigen	Colorectal carcinoma	*In vivo*
Iron oxide nanocrystals (Fe_3O_4)	Herceptin	Her-2/neu receptors	NIH3T6.7	*In vivo*
SPIO	Methotrexate	Folate receptor	Human cervical cancer cells	*In vitro*
SPIO	Chlorotoxin peptide	Membrane-bound matrix metalloproteinase-2 (MMP-2)	Rat glioma	*In vitro*
Biofunctional PEG-SPIO	Folic acid	Folate receptor	Human cervical cancer cells	*In vitro*
SPIO encapsulated with photodynamic agent	F3 peptide	Surface-localized tumor vasculature	Rat glioma	*In vivo*
HFn-IO	RGD4C	$\alpha_v\beta_3$ integrins	Melanoma cells	*In vitro*
SPIO	Luteinizing hormone releasing hormone (LHRH)	LHRH receptor	Breast cancer	*In vivo*
SPIO	CREKA peptide	Clotted plasma proteins	Breast cancer	*In vivo*
USPIO	Arg-Gly-Asp (RGD)	$\alpha_v\beta_3$ integrins	Human epidermoid carcinoma	*In vivo*
PEG-SPIO	Folic acid	Folate receptor	Human epithelial mouth carcinoma	*In vivo*
Streptavidin-SPIO	Antibody to prostate-specific membrane antigen (PSMA)	PSMA	Human prostate cancer cells	*In vitro*
Magnetism-engineered iron oxide (MEIO) nanoparticles	Herceptin	Her-2/neu receptors	NIH3T6.7	*In vivo*
PEG-IO	Chlorotoxin	Membrane-bound matrix metalloproteinase-2 (MMP-2)	Rat glioma	*In vivo*

Source: Peng [39] and references therein.

dose/gram, % ID/g) or organ activity (%ID/organ), the area under the curve (AUC) and their respective changes over time, predictions for an optimal imaging time, and thus radioactive half-life are possible [24, 47]. Similar calculations can be performed to obtain a "therapeutic figure of merit" (TFOM). Allometric analysis is used to obtain predictions for clinical trials of a novel probe based on preclinical data from animal models.

Most imaging modalities can yield quantitative data after careful calibration (Table 1.1). The previous paragraph illustrates the importance of quantification during early probe development and for clinical translation. Once an imaging probe has reached this step, quantitative image-based data analysis becomes even more relevant. Newly developed imaging probes need to be evaluated in patients, and sensitivity (ideally 100% = no false-negative examinations) and specificity (ideally 100% = no false-positive examinations) need to be established and compared to standard test methods (i.e., a "gold standard" such as biopsy/histopathology). Since molecular imaging is founded on the ability to quantify specific disease-related molecular profiles and target densities, the clinical goal is to go beyond mere detection of disease and to permit staging, restaging, and evaluation of response to treatment. To that end, image-derived quantitative parameters for evaluating the progression of a disease have been developed. For example, in oncology the "standard uptake value" (SUV) of a PET probe within a chosen "region of interest" (ROI)—the tumor—can be used as prognostic indicator [4, 48] and response to treatment can be assessed based on the change in SUV, often soon after the treatment since molecular changes precede changes detectable by anatomical or physiological imaging [49]. Regardless of the imaging modality, important parameters of an imaging protocol include (1) the imaging probe and its formulation, (2) the type and model of the scanner/detector, (3) patient selection and preparation, (4) data acquisition, (5) data processing, and (6) data analysis. All parameters need to be carefully controlled, recorded, and analyzed to yield results that are comparable over time and between different hospitals [50]. This is a prerequisite for meaningful results from clinical trials evaluating new imaging probes or new therapy regimens, and for subsequent clinical use based on reliable image acquisition and data handling protocols approved by regulatory agencies [49].

Ultimately, to be successful in clinical use, a new imaging probe needs to pass several tests: Is it better than competing diagnostic approaches? Does it have a cost-effective role in clinical management? Is the interpretation of the imaging data easy [4]? Once established, a well-studied imaging probe such as ^{18}F-FDG can then also play an important role in future drug development [51].

1.4.1 Nanoparticle-Based Probes

Molecular imaging can be performed with imaging probes of vastly different sizes. Entities can be the size of single atoms (e.g., a ^{18}F fluoride ion), small molecules (e.g., the modified glucose ^{18}F-FDG, the radiometal complex ^{99m}Tc-sestamibi), peptides, antibodies, or constructs approaching the dimension of small cells (e.g., micrometer-sized microbubbles [34]). Typical "nanoparticles" fall somewhere in the middle of this range. As outlined below, to be clinically useful the preferred size of nanoparticles is roughly between 10 and 100 nm [52]. Thus this classification covers compounds being similar in size to hemoglobin (6.5 nm), an antibody (12 nm), a hepatitis virus (45 nm), or an influenza virus (130 nm), although the constructs approaching the micrometer range are also commonly included in the definition. The nanoparticles themselves can extend in one to three dimensions, as depicted schematically in Figure 1.2, and show unique size- and shape-dependent properties that can be beneficial for imaging.

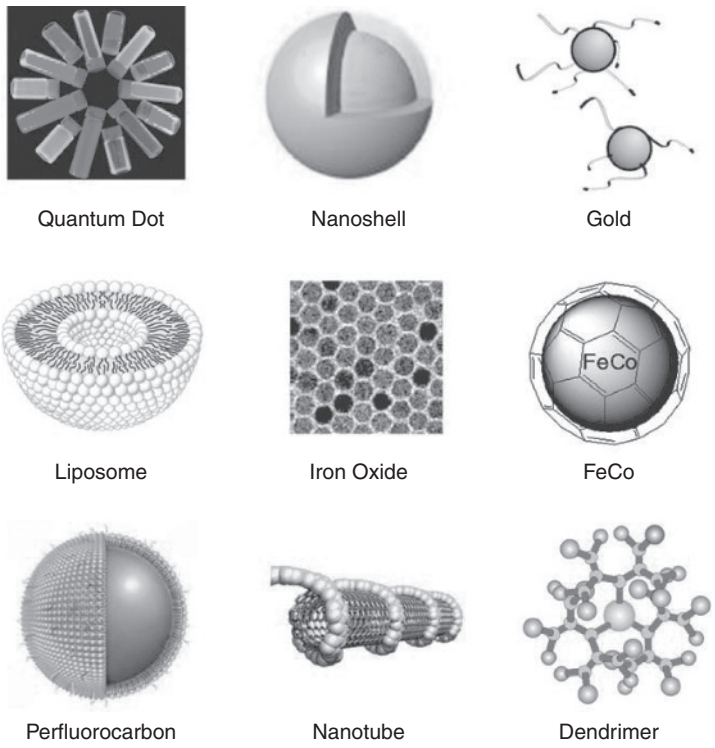

FIGURE 1.2 Schematic depictions of representative nanoparticles for targeted molecular imaging in living subjects. (Reproduced with permission from Cai [9].)

Nanoparticle-based probes are receiving considerable attention because the particles form a convenient platform for nanodiagnostics and nanomedicines that can combine different clinically relevant properties in a single unit. Each particle can carry highly specific targeting ligands, antibodies (for targeting or treatment), different imaging probes, drugs, or various combinations there of (Fig. 1.3). Depending on the nature of the particle, it itself can assume some of these roles. Examples include fluorescent quantum dots detectable by optical imaging, iron-based MRI contrast agents, carbon nanotubes used for targeted thermal ablation [53], and drug-carrying bubbles for ultrasound imaging. When an imaging

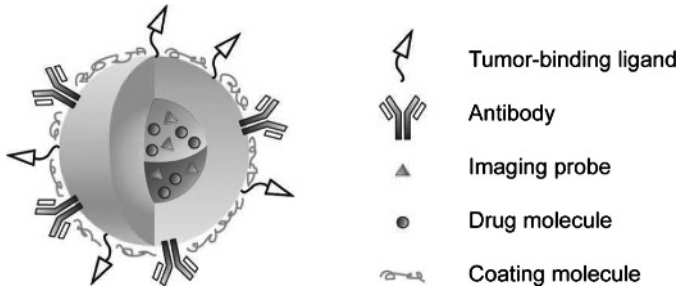

FIGURE 1.3 Schematic depiction of a targeted multifunctional nanoparticle carrying imaging probes, drugs, and antibodies. (Reproduced with permission from Rao [52].)

probe, that is, a diagnostic entity, is combined with a drug, the resulting compound is also called a "theranostic" or "theragnostic" [40, 54, 55]. Ideally, this integrated theranostic approach will permit diagnosis, targeted delivery of therapy, and monitoring of response to treatment Sumer 2008 [56]. By choosing the right combination of targeting moieties and therapeutic components, the theranostic can home in on multiple markers and target cell subpopulations, thereby providing a tool to address disease heterogeneity and adaptive resistance. The treatment can, if necessary, quickly be adjusted based on the rapid feedback obtained. Although still in its early stages, the hope is that this approach will allow true "personalized medicine" based on individualized, molecular diagnosis within a heterogeneous disease and patient population, something that cannot be accomplished by taking small biopsy samples or following standardized "one-dose-fits-all" protocols.

As already alluded to in the previous paragraphs, nanoparticle-based probes offer several advantages over standard probes Sanvicens 2008 [57, 58].

First, the size of nanoparticles allows them to carry a large number of targeting ligands. The binding behavior is influenced by the ligands' affinities, their density, and by the combination of the chosen ligands. Because of the resulting multivalent binding ("avidity"), a nanoparticle can exhibit high-affinity binding even though low-affinity ligands were employed [59] and different receptors may be targeted simultaneously.

Second, moieties for multiple imaging modalities can be combined onto a single particle. This makes the nanoparticles amendable to dual-/multimodality imaging and allows one to draw on the strengths of different imaging modalities (e.g., high resolution and high sensitivity, Table 1.1). For a comparable small-molecule probe, achieving desirable signal strengths for each of the different imaging modalities can be challenging because the ratio of the different imaging moieties (e.g., an optical dye molecule and a radioisotope-bearing prosthetic group) cannot be easily changed [60] and the introduction of additional groups can significantly affect pharmacokinetics. By contrast, the ratio of the different moieties can be tailored more easily on nanoparticles, be it to achieve simultaneous detection in all modalities, or to use a high-sensitivity "beacon" (e.g., a PET-isotope) to trace low-sensitivity particles (e.g., MRI particles) at very low concentrations [61, 62].

Third, nanoparticles used as theranostics can carry large numbers of therapeutic entities like small molecules or peptides. Depending on the type of nanoparticle used, these payloads can be stowed away in the core, eliminating deleterious interference with pharmacokinetics and biodistribution. In addition, different types of drug molecules can be combined in a single particle.

Fourth, drug-delivery kinetics can be tuned for a particular target and monitored using molecular imaging. A "controlled release" after delivery to the target helps to protect the rest of the body from harmful side effects, while at the same time increasing the "effective dose" in the target tissue. The drugs may be released by a microenvironmental stimulus such as pH or enzymes [63] or by external stimuli. An example for the latter are drug-carrying microbubbles that can be tracked by conventional ultrasound and fragmented using destructive high-intensity US pulses, releasing the drug in the target region [34]. When drug delivery directly into the cells is desired [64], multimodality nanoparticles can be modified for efficient endocytosis by decoration with cell-penetrating groups such as Tat-peptides [65, 66] and tracked by molecular imaging. Furthermore, there is evidence that nanoparticles may be able to sidestep multidrug resistance involving protein efflux pumps [57].

Fifth, nanoparticle pharmacokinetics can be modified with surface modifications. To improve the pharmacokinetic properties and *in vivo* stability, the particles are oftentimes

coated with biocompatible polymers such as polyethylene glycol (PEG) or the polysaccharide dextran. This coating effectively "hides" the particles from detection by the reticuloendothelial system (RES), which would otherwise rapidly eliminate them by opsonization and phagocytosis [63]. All these modifications have to be accomplished while keeping the hydrodynamic (HD) size roughly between 10 and 100 nm. If particles fall below the lower limit, renal filtration provides a rapid way of elimination, while, on the other hand, hepatic and splenic elimination becomes increasingly efficient for particles greater than 100 nm [46]. For solid tumors, effective delivery to the target tissue beyond the vascular compartment is another reason for the upper size limit: since the gaps in leaky vasculature are about 400 nm, extravasation is most efficient for particles well below this limit [67]. This fact also explains why microbubble-based US imaging is largely confined to the vascular compartment; for other—smaller—nanoparticles, this passive targeting phenomenon, termed "enhanced permeation and retention" (EPR) effect, together with a lack of efficient lymphatic drainage, represents an important way of tumor-directed delivery, particularly for smaller tumors [68].

Besides the hydrodynamic size, the charge of the nanoparticle can also affect pharmacokinetics and biodistribution. Ideally, a nanoparticle should exhibit a near neutral charge since positively charged particles can form aggregates with negatively charged plasma proteins, while negatively charged particles demonstrate increased liver uptake [69]. The positive effects of nanoparticle coatings on pharmacokinetics include shielding of surface charges and surface chemistry. The commercial availability of PEG in a wide range of lengths and modifications has made it particularly popular for fine-tuning of these pharmacokinetic properties. For example, one study showed that after relatively small, nontargeted quantum dots with identical 3.2-nm diameter InAs(ZnS) core were coated with PEG-chains of various lengths (PEG2 to PEG22), resulting in HD sizes ranging from 5 to 16 nm, the biodistribution and clearance characteristics varied widely [70]. Expectedly, PEGylation improved hydrophilicity, protected from opsonization, and circulation times in the blood increased with increasing chain length. In addition, by simply increasing the length of the PEG units, major organ uptake shifted from liver over kidneys and bladder to pancreas, intestine, and lymph nodes.

However, it has to be underscored that in the study cited above, the quantum dots did not bear any specific targeting moiety. Fortunately for *targeted* nanoparticles, recent data indicate that the presence of targeting moieties may minimize the influences of other nanoparticle properties *in vivo* [71]: a preclinical study compared different carriers (linear polymer, dendrimer, and liposome) carrying an anticancer drug (paclitaxel) and/or an imaging probe (Cy5.5) in conjunction with a targeting moiety (a LHRH peptide). Notably, the authors conclude "that the architecture, composition, size and molecular mass of the receptor-targeted drug nanocarriers can be selected based on other than anticancer efficacy considerations (cost, type of active ingredients, difficulties in production, stability, patient compliance, etc.) ensuring that *the high efficacy and low adverse side effects could be achieved automatically by tumor targeting*" [emphasis added] [71]. If similar results are found in other studies, the focus might shift toward careful selection of the targeting ligand(s) while allowing a high degree of flexibility for the underlying platform [72].

1.4.2 Challenges for Nanoparticle-Based Imaging Probes

The body of work produced to date has demonstrated the promising potential of nanoparticle-based molecular imaging agents [9, 11, 12]. At the same time, the studies

have shown some of the accompanying challenges Sanvicens 2008 [57]. They chiefly fall within three basic areas: compound preparation, toxicity, and pharmacokinetics/pharmacodynamics. Understanding and addressing these challenges will also be highly important to gain the regulatory approval necessary for rapid and successful translation into the clinic. Some of the challenges are described next.

1. *Size Control and Batch-to-Batch Reproducibility.* In contrast to small-molecule probes, achieving good control over the size and precise composition of nanoparticles is more challenging. But since pharmacokinetics and, for theranostics, pharmacodynamics can be significantly influenced by these factors, gaining a thorough understanding of these manufacturing parameters and their *in vivo* consequences is crucial [46, 69, 71]. Taking magnetic nanoparticles used for MRI as an example, it is well known that the (superpara)magnetic properties are size dependent as surface effects play an increasing role for smaller particles and that magnetic properties can vary significantly depending on production chemistry [32, 73].

2. *Particle Stability During Storage and Formulation.* Because of their size and surface properties, nanoparticles may aggregate over time. This and other deleterious changes such as decomposition and oxidation have to be evaluated.

3. *Toxicity and Immune Response.* The composition and shape of the nanoparticles can potentially have toxic effects. For example, many quantum dots popular for optical fluorescence imaging contain cadmium, lead, or selenium [74]. Magnetic nanoparticles used for MRI may contain gadolinium, cobalt, or nickel [31, 75]. Even if these toxic elements are shielded from direct contact with the *in vivo* environment by protective coatings, they may eventually leach out if residence times in the body are long. For carbon nanotubes, their shape rather than their composition could be cause for concern. Similar to quartz and asbestos, they have been shown to be capable of causing chronic inflammation and fibrosis [76]. In addition, while coatings are useful for shielding the core of the nanoparticles from the immune system, if antibodies are used for targeting, they necessarily need to be exposed to the *in vivo* environment, thus posing a risk for an immune response. Fortunately, less immunogenic antibody-derived targeting moieties may be available and biodegradable low-toxicity nanoparticles are being developed [72].

4. *Control Over Pharmacokinetics/Pharmacodynamics.* Nanoparticles demonstrate long blood circulation times and, because of their size, show a tendency to undergo opsonization and clear the body via the liver and spleen. Clearance through the reticuloendothelial system is slower than the excretion in the urine encountered for many small molecules [69]. The longer residence time in excretory organs may not be a significant concern for imaging probes administered in trace amount, but could become pharmacodynamically relevant for theranostics carrying highly potent drug molecules or therapeutic radioisotopes.

In the end, solving some of these challenges could be easier than it appears at present. As the recent study by Saad and co-workers has indicated [71], depending on which information is desired about the target, choosing the imaging modality (or modalities) and targeting moiety may be the most important factors to consider when designing the imaging agent, while leaving considerable flexibility for the underlying platform. Specifically, the authors found "that tumor-specific targeting minimized the differences between nanocarriers of distinct architecture, size, mass, and composition" [71]. If these findings represent a

general principle, they could have wide-ranging implications for the rapidly growing field of nanoparticle-based diagnostic and treatment tools. Thus despite the seemingly overwhelming number of potential combinations of sizes, shapes, compositions, surface coatings, targeting moieties, imaging modalities, functional groups, and potential drug molecules, in the future the challenge may not be so much trying to *discover* a molecular imaging agent for a particular target, but rather to *assemble the best combination of components* from the choices available in the toolbox.

REFERENCES

1. Ludwig, J. A.; Weinstein, J. N. Biomarkers in cancer staging, prognosis and treatment selection. *Nat. Rev. Cancer* **2005**, *5*, 845–856.
2. Tan, A. R.; Swain, S. M. Ongoing adjuvant trials with trastuzumab in breast cancer. *Semin. Oncol.* **2003**, *30*, 54–64.
3. Menard, S.; Casalini, P.; Campiglio, M.; Pupa, S. M.; Tagliabue, E. Role of HER2/neu in tumor progression and therapy. *Cell. Mol. Life Sci.* **2004**, *61*, 2965–2978.
4. Hoh, C. K. Clinical use of FDG PET. *Nucl. Med. Biol.* **2007**, *34*, 737–742.
5. Cherry, S. R. Multimodality *in vivo* imaging systems: twice the power or double the trouble? *Annu. Rev. Biomed. Eng.* **2006**, *8*, 35–62.
6. Society of Nuclear Medicine, Glossary of Molecular Imaging Terms. Available at http://www.molecularimagingcenter.org/index.cfm?PageID=7834 (accessed April 3, 2009)
7. Baert, A. L. In *Encyclopedia of Diagnostic Imaging*. Springer-Verlag: New York, 2008, p. 1618.
8. Bloch, S. H.; Dayton, P. A.; Ferrara, K. W. Targeted imaging using ultrasound contrast agents. *IEEE Eng. Med. Biol. Mag.* **2004**, *23*, 18–29.
9. Cai, W. B.; Chen, X. Y. Nanoplatforms for targeted molecular imaging in living subjects. *Small* **2007**, *3*, 1840–1854.
10. Ferrara, K. W. Driving delivery vehicles with ultrasound. *Adv. Drug Deliv. Rev.* **2008**, *60*, 1097–1102.
11. Willmann, J. K.; van Bruggen, N.; Dinkelborg, I. M.; Gambhir, S. S. Molecular imaging in drug development. *Nat. Rev. Drug Discov.* **2008**, *7*, 591–607.
12. Weissleder, R.; Pittet, M. J. Imaging in the era of molecular oncology. *Nature* **2008**, *452*, 580–589.
13. Shah, C.; Patton, J. A.; Sandler, M. P. How much CT is needed in nuclear medicine. *Eur. J. Nucl. Med. Mol. Imaging* **2008**, *35*, 1759–1760.
14. von Schulthess, G. K.; Schlemmer, H. P. W. A look ahead: PET/MR versus PET/CT. *Eur. J. Nucl. Med. Mol. Imaging* **2009**, *36*, 3–9.
15. Moser, E.; Stadlbauer, A.; Windischberger, C.; Quick, H. H.; Ladd, M. E. Magnetic resonance imaging methodology. *Eur. J. Nucl. Med. Mol. Imaging* **2009**, *36*, 30–41.
16. Pichler, B. J.; Wehrl, H. F.; Judenhofer, M. S. Latest advances in molecular imaging instrumentation. *J. Nucl. Med.* **2008**, *49*, 5S–23S.
17. Ntziachristos, V.; Chance, B. Probing physiology and molecular function using optical imaging: applications to breast cancer. *Breast Cancer Res.* **2001**, *3*, 41–46.
18. Rudin, M.; Weissleder, R. Molecular imaging in drug discovery and development. *Nat. Rev. Drug Discov.* **2003**, *2*, 123–131.
19. So, M. K.; Xu, C. J.; Loening, A. M.; Gambhir, S. S.; Rao, J. H. Self-illuminating quantum dot conjugates for in vivo imaging. *Nat. Biotechnol.* **2006**, *24*, 339–343.

20. Mather, S. Molecular imaging with bioconjugates in mouse models of cancer. *Bioconjug. Chem.* **2009**, *20*, 631–643.
21. Levenson, R. M.; Mansfield, J. R. Multispectral imaging in biology and medicine: slices of life. *Cytometry A* **2006**, *69A*, 748–758.
22. Evans, C. L.; Potma, E. O.; Puoris'haag, M.; et al. Chemical imaging of tissue in vivo with video-rate coherent anti-Stokes Raman scattering microscopy. *Proc. Natl. Acad. Sci. U.S.A.* **2005**, *102*, 16807–16812.
23. Fujimoto, J. G. Optical coherence tomography for ultrahigh resolution in vivo imaging. *Nat. Biotechnol.* **2003**, *21*, 1361–1367.
24. Williams, L. E.; Lopatin, G.; Kaplan, D. D.; Liu, A.; Wong, J. Y. C. Update on selection of optimal radiopharmaceuticals for clinical trials. *Cancer Biother. Radiopharm.* **2008**, *23*, 797–806.
25. Cherry, S. R. The 2006 Henry N. Wagner lecture: of mice and men (and positrons)—advances in PET imaging technology. *J. Nucl. Med.* **2006**, *47*, 1735–1745.
26. Levin, C. S.; Hoffman, E. J. Calculation of positron range and its effect on the fundamental limit of positron emission tomography system spatial resolution. *Phys. Med. Biol.* **1999**, *44*, 781–799.
27. Lecomte, R. Technology challenges in small animal PET imaging. *Nucl. Instrum. Methods Phys. Res. A—Accelerators Spectrometers Detectors* and *Associated Equipment* **2004**, *527*, 157–165.
28. Nayak, T. K.; Brechbiel, M. W. Radioimmunoimaging with longer-lived positron-emitting radionuclides: potentials and challenges. *Bioconjug. Chem.* **2009**, *20*, 825–841.
29. Ambrosini, V.; Quarta, C.; Nanni, C.; et al. Small animal PET in oncology: the road from bench to bedside. *Cancer Biotherapy Radiopharm.* **2009**, *24*, 277–285.
30. Na, H. B.; Lee, J. H.; An, K. J.; et al. Development of a T1 contrast agent for magnetic resonance imaging using MnO nanoparticles. *Angew. Chem. Int. Ed.* **2007**, *46*, 5397–5401.
31. Castelli, D. D.; Gianolio, F.; Crich, S. G.; Terreno, E.; Aime, S. Metal containing nanosized systems for MR—molecular imaging applications. *Coord. Chem. Rev.* **2008**, *252*, 2424–2443.
32. Sun, C.; Lee, J. S. H.; Zhang, M. Q. Magnetic nanoparticles in MR imaging and drug delivery. *Adv. Drug Deliv. Rev.* **2008**, *60*, 1252–1265.
33. Jenkinson, M. D.; du Plessis, D. G.; Walker, C.; Smith, T. S. Advanced MRI in the management of adult gliomas. *Br. J. Neurosurg.* **2007**, *21*, 550–561.
34. Ferrara, K.; Pollard, R.; Borden, M. Ultrasound microbubble contrast agents: fundamentals and application to gene and drug delivery. *Annu. Rev. Biomed. Eng.* **2007**, *9*, 415–447.
35. Zielhuis, S. W.; Nijsen, J. F.; Seppenwoolde, J. H.; et al. Lanthanide bearing microparticulate systems for multi-modality imaging and targeted therapy of cancer. *Curr. Med. Chem. Anticancer Agents* **2005**, *5*, 303–313.
36. Rabin, O.; Perez, J. M.; Grimm, J.; Wojtkiewicz, G.; Weissleder, R. An X-ray computed tomography imaging agent based on long-circulating bismuth sulphide nanoparticles. *Nat. Mater.* **2006**, *5*, 118–122.
37. Popovtzer, R.; Agrawal, A.; Kotov, N. A.; et al. Targeted gold nanoparticles enable molecular CT imaging of cancer. *Nano Lett.* **2008**, *8*, 4593–4596.
38. Gambhir, S. S. Molecular imaging of cancer with positron emission tomography. *Nat. Rev. Cancer* **2002**, *2*, 683–693.
39. Peng, X. H.; Qian, X. M.; Mao, H.; et al. Targeted magnetic iron oxide nanoparticles for tumor imaging and therapy. *Int. J. Nanomed.* **2008**, *3*, 311–321.
40. Del Vecchio, S.; Zanneti, A.; Fonti, R.; Pace, L.; Salvatore, M. Nuclear imaging in cancer theranostics. *Q. J. Nucl. Med. Mol. Imaging* **2007**, *51*, 152–163.
41. Daniel, K. D.; Kim, G. Y.; Vassiliou, C. C.; et al. Implantable diagnostic device for cancer monitoring. *Biosensors & Bioelectronics* **2009**, *24*, 3252–3257.

42. Gross, S.; Piwnica-Worms, D. Spying on cancer: molecular imaging in vivo with genetically encoded reporters. *Cancer Cell* **2005**, *7*, 5–15.
43. Barrett, T.; Choyke, P. L.; Kobayashi, H. Imaging of the lymphatic system: new horizons. *Contrast Media & Mol. Imaging* **2006**, *1*, 230–245.
44. Hausner, S. H.; Abbey, C. K.; Bold, R. J.; et al. Targeted in vivo imaging of integrin alpha(v)beta(6) with an improved radiotracer and its relevance in a pancreatic tumor model. *Cancer Res.* **2009**, *69*, 5843–5850.
45. Ito, H.; Inoue, K.; Goto, R.; et al. Database of normal human cerebral blood flow measured by SPECT: I. Comparison between I-123-IMP, Tc-99m-HMPAO, and Tc-99m-ECD as referred with O-15 labeled water PET and voxel-based morphometry. *Ann. Nucl. Med.* **2006**, *20*, 131–138.
46. Alexis, F.; Pridgen, F.; Molnar, L. K.; Farokhzad, O. C. Factors affecting the clearance and biodistribution of polymeric nanoparticles. *Mol. Pharm.* **2008**, *5*, 505–515.
47. Williams, L. E.; Wu, A. M.; Yazaki, P. J.; et al. Numerical selection of optimal tumor imaging agents with application to engineered antibodies. *Cancer Biother. Radiopharm.* **2001**, *16*, 25–35.
48. Weber, W. A. Positron emission tomography as an imaging biomarker. *J. Clin. Oncol.* **2006**, *24*, 3282–3292.
49. Krause, B. J.; Herrmann, K.; Wieder, H.; zum Buschenfelde, C. M. ^{18}F-FDG PET and ^{18}F-FDG PET/CT for assessing response to therapy in esophageal cancer. *J. Nucl. Med.* **2009**, *50*(Suppl 1), 89S–96S.
50. McLennan, G.; Clarke, L.; Hohl, R. J. Imaging as a biomarker for therapy response: cancer as a prototype for the creation of research resources. *Clin. Pharmacol. Ther.* **2008**, *84*, 433–436.
51. Weber, W. A.; Czernin, J.; Phelps, M. F.; Herschman, H. R. Technology insight: novel imaging of molecular targets is an emerging area crucial to the development of targeted drugs. *Nat. Clin. Practice Oncol.* **2008**, *5*, 44–54.
52. Rao, J. H. Shedding light on tumors using nanoparticles. *ACS Nano* **2008**, *2*, 1984–1986.
53. Kim, K. Y. Nanotechnology platforms and physiological challenges for cancer therapeutics. *Nanomed. Nanotechnol. Biol. Med.* **2007**, *3*, 103–110.
54. Warner, S. Diagnostics plus therapy = theranostics. *Scientist* **2004**, *18*, 38–39.
55. Pene, F.; Courtine, E.; Cariou, A.; Mira, J. P. Toward theragnostics. *Crit. Care Med.* **2009**, *37*, S50–S58.
56. Sumer, B.; Gao, J. M. Theranostic nanomedicine for cancer. *Nanomedicine* **2008**, *3*, 137–140.
57. Sanvicens, N.; Marco, M. P. Multifunctional nanoparticles—properties and prospects for their use in human medicine. *Trends Biotechnol.* **2008**, *26*, 425–433.
58. Davis, M. E.; Chen, Z.; Shin, D. M. Nanoparticle therapeutics: an emerging treatment modality for cancer. *Nat. Rev. Drug Discov.* **2008**, *7*, 771–782.
59. Hong, S.; Leroueil, P. R.; Majoros, I. J.; et al. The binding avidity of a nanoparticle-based multivalent targeted drug delivery platform. *Chem. Biol.* **2007**, *14*, 107–115.
60. Edwards, W. B.; Akers, W. J.; Ye, Y. P.; et al. Multimodal imaging of integrin receptor-positive tumors by bioluminescence, fluorescence, gamma scintigraphy, and single-photon emission computed tomography using a cyclic RGD peptide labeled with a rear-infrared fluorescent dye and a radionuclide. *Mol. Imaging* **2009**, *8*, 101–110.
61. Devaraj, N. K.; Keliher, F. I.; Thurber, G. M.; Nahrendorf, M.; Weissleder, R. F-18 labeled nanoparticles for in vivo PET-CT imaging. *Bioconjug. Chem.* **2009**, *20*, 397–401.
62. Lee, S.; Chen, X. Y. Dual-modality probes for in vivo molecular imaging. *Mol. Imaging* **2009**, *8*, 87–100.
63. Gullotti, E.; Yeo, Y. Extracellularly activated nanocarriers: a new paradigm of tumor targeted drug delivery. *Mol. Pharm.* **2009**, *6*, 1041–1051.

64. Bae, Y. H. Drug targeting and tumor heterogeneity. *J. Control. Release* **2009**, *133*, 2–3.
65. Koch, A. M.; Reynolds, F.; Kircher, M. F.; et al. Uptake and metabolism of a dual fluorochrome tat-nanoparticle in HeLa cells. *Bioconjug. Chem.* **2003**, *14*, 1115–1121.
66. Bullok, K. E.; Gammon, S. T.; Violini, S.; et al. Permeation peptide conjugates for in vivo molecular imaging applications. *Mol. Imaging* **2006**, *5*, 1–15.
67. Gabizon, A. A.; Shmeeda, H.; Zalipsky, S. Pros and cons of the liposome platform in cancer drug targeting. *J. Liposome Res.* **2006**, *16*, 175–183.
68. Duncan, R. The dawning era of polymer therapeutics. *Nat. Rev. Drug Discov.* **2003**, *2*, 347–360.
69. Li, S. D.; Huang, L. Pharmacokinetics and biodistribution of nanoparticles. *Mol. Pharm.* **2008**, *5*, 496–504.
70. Choi, H. S.; Ipe, B. I.; Misra, P.; et al. Tissue- and organ-selective biodistribution of NIR fluorescent quantum dots. *Nano Lett.* **2009**, *9*, 2354–2359.
71. Saad, M.; Garbuzenko, O. B.; Ber, E.; et al. Receptor targeted polymers, dendrimers, liposomes: Which nanocarrier is the most efficient for tumor-specific treatment and imaging? *J. Controll. Release* **2008**, *130*, 107–114.
72. Park, J. H.; Gu, L.; von Maltzahn, G.; et al. Biodegradable luminescent porous silicon nanoparticles for in vivo applications. *Nat. Mater.* **2009**, *8*, 331–336.
73. Lu, A. H.; Salabas, E. L.; Schuth, F. Magnetic nanoparticles: synthesis, protection, functionalization, and application. *Angew. Chem. Int. Ed.* **2007**, *46*, 1222–1244.
74. Resch-Genger, U.; Grabolle, M.; Cavaliere-Jaricot, S.; Nitschke, R.; Nann, T. Quantum dots versus organic dyes as fluorescent labels. *Nat. Methods* **2008**, *5*, 763–775.
75. Shultz, M. D.; Calvin, S.; Fatouros, P. P.; Morrison, S. A.; Carpenter, E. E. Enhanced ferrite nanoparticles as MRI contrast agents. *J. Magn. Magn. Mater.* **2007**, *311*, 464–468.
76. Lam, C. W.; James, J. T.; McCluskey, R.; Arepalli, S.; Hunter, R. L. A review of carbon nanotube toxicity and assessment of potential occupational and environmental health risks. *Crit. Rev. Toxicol.* **2006**, *36*, 189–217.